Generating stationary entangled states in superconducting qubits

Jing Zhang,[1,2,*] Yu-xi Liu,[1,3] Chun-Wen Li,[2] Tzyh-Jong Tarn,[4] and Franco Nori[1,3,5]
[1]*Advanced Science Institute, The Institute of Physical and Chemical Research (RIKEN), Wako-shi, Saitama 351-0198, Japan*
[2]*Department of Automation, Tsinghua University, Beijing 100084, People's Republic of China*
[3]*CREST, Japan Science and Technology Agency (JST), Kawaguchi, Saitama 332-0012, Japan*
[4]*Department of Electrical and Systems Engineering, Washington University, St. Louis, Missouri 63130, USA*
[5]*Department of Physics, Center for Theoretical Physics, Center for the Study of Complex Systems, The University of Michigan, Ann Arbor, Michigan 48109-1040, USA*
(Received 22 August 2008; published 11 May 2009)

When a two-qubit system is initially maximally entangled, two independent decoherence channels, one per qubit, would greatly reduce the entanglement of the two-qubit system when it reaches its stationary state. We propose a method on how to minimize such a loss of entanglement in open quantum systems. We find that the quantum entanglement of general two-qubit systems with controllable parameters can be controlled by tuning both the single-qubit parameters and the two-qubit coupling strengths. Indeed, the maximum fidelity $F_{\max}$ between the stationary entangled state, ρ_∞, and the maximally entangled state, ρ_m, can be about $2/3 \approx \max\{\mathrm{tr}(\rho_\infty \rho_m)\} = F_{\max}$, corresponding to a maximum stationary concurrence, $C_{\max}$, of about $1/3 \approx C(\rho_\infty) = C_{\max}$. This is significant because the quantum entanglement of the two-qubit system can be produced and kept, even for a long time. We apply our proposal to several types of two-qubit superconducting circuits and show how the entanglement of these two-qubit circuits can be optimized by varying experimentally controllable parameters.

DOI: 10.1103/PhysRevA.79.052308 PACS number(s): 03.67.Pp, 85.25.−j, 03.67.Lx

I. INTRODUCTION

Quantum information processing using superconducting qubits (see, e.g., [1–4]) has made remarkable advances in the past few years. One-qubit and two-qubit quantum circuits (see, e.g., [5–11]) have been realized experimentally in superconducting systems. One of the most important issues in quantum information processing is how to couple two qubits, which has been widely studied theoretically and experimentally in superconducting quantum circuits (see, e.g., [5–27]). To couple two qubits, there are two types of approaches: (1) direct coupling and (2) indirect coupling. Examples of qubit-qubit direct coupling include, e.g., capacitively coupled charge qubits [5,6] or inductively coupled flux qubits [8,9,12]. Examples of indirect coupling include, e.g., qubit-qubit coupling via a quantum *LC* oscillator or an inductance [16–19], a Josephson junction or an extra superconducting qubit acting as a coupler [21,22], a nanomechanical oscillator [23], or a transmission line resonator [24–26]. The main merit of indirect coupling is that any two qubits can be selectively coupled in a controllable way (see, e.g., [27]). By tuning some control parameters, one can continuously adjust the coupling strengths between qubits, which can be further used to switch between one-qubit and two-qubit operations.

Although maximally entangled states can be prepared via two-qubit quantum operations realized by the time evolution of either directly or indirectly coupled two-qubit superconducting quantum circuits [28], the entanglement of the prepared quantum states would be greatly reduced in open environments. Thus, it is important to study how to prepare entangled states under decoherence and dissipation, which leads to the so-called stationary entanglement production strategies [29–31]. Most of the proposed stationary entanglement production strategies utilize a *common* dissipative environment [29,30], e.g., a heat bath. Specifically, a common dissipative environment would lead to a collective decoherence channel which may induce a so-called decoherence-free subspace [31] to produce and protect special two-qubit entangled states.

Although the dissipation-induced entanglement production strategies based on collective dissipative environments have been well developed, it is difficult to obtain perfect collective decoherence channels in experimental solid-state systems (e.g., superconducting quantum circuits). The decoherence channels for different qubits in these systems are sometimes *independent* or a mixture of independent and collective decoherence channels. In contrast to the collective decoherence channels, independent decoherence channels usually lead to disentanglement [32]. This loss of entanglement cannot be recovered by local operations and classical communications, when the two qubits reach their stationary states. Even worse, a mixture of the "independent decoherence" and the "collective decoherence" channels may destroy the decoherence-free subspace and lead to a failure of the entanglement production. Thus, it is challenging to produce stationary entanglement in the presence of such a dissipative environment, with independent decoherence channels acting on each qubit.

Compared to the transient entanglement produced, e.g., by two-qubit quantum operations, the stationary entanglement would not oscillate as the transient entanglement and could be preserved for a long time even in the presence of decoherence. Also, the stationary entanglement is more "robust" on the initial-state preparation (e.g., the stationary entanglement we obtain in this paper is independent of the system initial state), but the transient entanglement strongly

*jing-zhang@mail.tsinghua.edu.cn

depends on the initial states and the time duration of the dynamical evolution. Therefore, the dissipation-induced stationary entanglement is more stable and "robust" than the transient entanglement prepared by the system time evolution with different initial states.

Although the stationary entanglement has many benefits, we would like to raise the following questions: (i) the level of entanglement remaining in an open system that reaches its steady state and (ii) if the stationary entangled state can be used for quantum information processing. In this work, we first study a general theory on two-qubit entanglement when the two-qubit system reaches its steady state. We find that the stationary state of this system includes a component of the maximally entangled state. The weight of this component can be tuned by either single-qubit or two-qubit parameters, by which the maximum fidelity between the maximally entangled state and the stationary state can be achieved. Although the obtained stationary entanglement nay not be high enough to be applied directly to quantum information processing, it could be increased by introducing an additional entanglement-purification process. We further apply our general theory to study several examples of superconducting qubits.

This paper is organized as follows: in Sec. II we present our main results for general two-qubit systems. The entanglement production for directly and indirectly coupled superconducting qubits via an inductive or a capacitive coupler is presented in Secs. III and IV. In Sec. V, we study the entanglement production in superconducting qubit circuits interacting with controllable squeezed modes in cavities or resonators (e.g., circuit QED). Conclusions and discussions are given in Sec. VI.

II. GENERAL RESULTS

We consider two coupled qubits with a general Hamiltonian

$$H_A = \mu_1[\exp(-i\theta_1)\sigma_+^{(1)}\sigma_+^{(2)} + \exp(i\theta_1)\sigma_-^{(1)}\sigma_-^{(2)}] + \mu_2[\exp(-i\theta_2)\sigma_+^{(1)}\sigma_-^{(2)} + \exp(i\theta_2)\sigma_-^{(1)}\sigma_+^{(2)}] + \sum_{j=1}^{2}\frac{\omega_{aj}}{2}\sigma_z^{(j)}, \quad (1)$$

where the Planck constant $\hbar$ is assumed to be 1. Here, $\sigma_\pm^{(j)} = \sigma_x^{(j)} \pm i\sigma_y^{(j)}$, and $\sigma_x^{(j)}, \sigma_y^{(j)}, \sigma_z^{(j)}$ are the ladder and Pauli operators of the jth qubit. The frequency of the jth qubit is denoted by ω_{aj}. The real coefficients μ_1 (with phase θ_1) and μ_2 (with phase θ_2) correspond to the $\sigma_-^{(1)}\sigma_-^{(2)}$ and $\sigma_-^{(1)}\sigma_+^{(2)}$ coupling strengths, which are assumed to be tunable parameters.

The qubits also interact with uncontrollable degrees of freedom in the environment (see, e.g., Refs. [33–35]). If the two qubits interact independently with their own environments, then, under the Born-Markov approximation [36], we can obtain the following master equation:

$$\dot{\rho} = -i[H_A,\rho] + \sum_{j=1}^{2}\Gamma_1\mathcal{D}[\sigma_-^{(j)}]\rho + \sum_{j=1}^{2}2\Gamma_\phi\mathcal{D}[\sigma_z^{(j)}]\rho, \quad (2)$$

where the superoperator $\mathcal{D}[L]\rho$ is defined as

$$\mathcal{D}[L]\rho = L\rho L^\dagger - \frac{1}{2}L^\dagger L\rho - \frac{1}{2}\rho L^\dagger L,$$

and Γ_1 and Γ_ϕ represent the relaxation and pure dephasing rates for each qubit, respectively. In order to simplify our discussions, it is assumed that the two qubits have the same relaxation and pure dephasing rates.

Below, we will use the concurrence $C(\rho)$:

$$C(\rho) = \max\{\lambda_1 - \lambda_2 - \lambda_3 - \lambda_4, 0\}, \quad (3)$$

to quantify the quantum entanglement between the two qubits (see Ref. [37]), where the λ_i's are the square roots of the eigenvalues, in decreasing order, of the matrix

$$M = \rho(\sigma_y^{(1)}\sigma_y^{(2)})\rho^*(\sigma_y^{(1)}\sigma_y^{(2)}),$$

and ρ^* is the complex conjugate of the density matrix ρ.

If the two qubits do not interact with each other, i.e., $\mu_1 = \mu_2 = 0$ in Eq. (2), the stationary state of the two qubits should be the ground state $\rho_\infty^u = |00\rangle\langle 00|$ (see, e.g., [32]), where the superscript "u" refers to "uncontrolled" qubit system. Since $\rho_\infty^u = |00\rangle\langle 00|$ is a separable state, no stationary entanglement is produced even if the initial state is prepared to be a maximally entangled state. However, the following discussions show that the stationary entanglement can be produced by tuning the interaction strength μ_1 and the single-qubit frequencies ω_{aj} in Eq. (1).

A. Strong interaction regime: $\mu_i \sim 10^{-1}(\omega_{a1} + \omega_{a2})$

Let us now study the regime where the coupling strengths μ_1 and μ_2 are about 1 order of magnitude smaller than the sum of the two single-qubit frequencies: $\Omega = \omega_{a1} + \omega_{a2}$, and the phases θ_1, θ_2 are both time-independent parameters. For such systems, we have the following results:

The solution $\rho(t)$ of Eq. (2) tends to a stationary state

$$\rho_\infty = p\rho_m + (1-p)\rho_s \quad (4)$$

as a convex combination of a maximally entangled state ρ_m:

$$\rho_m = \frac{1}{2}(|00\rangle + e^{i(\theta_1-\phi)}|11\rangle)(\langle 00| + e^{-i(\theta_1-\phi)}\langle 11|) = \frac{1}{2}\begin{pmatrix} 1 & & & \exp[-i(\theta_1-\phi)] \\ & 0 & & \\ & & 0 & \\ \exp[i(\theta_1-\phi)] & & & 1 \end{pmatrix}$$

and a diagonal separable state ρ_s:

$$\rho_s = \begin{pmatrix} 1-3\beta & & & \\ & \beta & & \\ & & \beta & \\ & & & \beta \end{pmatrix},$$

where

$$\beta = \frac{1}{8}\left(1 - \sqrt{1 - \frac{8\Gamma_2}{\Gamma_1}p^2}\right).$$

The subscript "m" is an abbreviation of "maximally entangled," and the subscript "s" refers to "separable." $|0\rangle, |1\rangle$

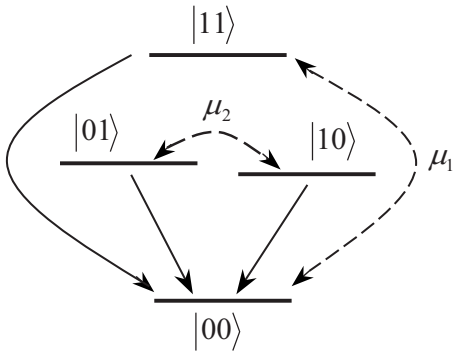

FIG. 1. Schematic diagram of the energy transitions between the four states: $|00\rangle$, $|11\rangle$, $|10\rangle$, and $|01\rangle$. The solid arrows denote the decays caused by independent relaxation and dephasing channels. The dashed arrows represent the coherent superpositions caused by the interactions between qubits (with interaction strengths μ_1 and μ_2, respectively).

are the two eigenstates of a single qubit. The parameters p, ϕ can be expressed as

$$p = \frac{\sqrt{\Omega^2 + 64\Gamma_2^2}/8\mu_1}{2\Gamma_2/\Gamma_1 + (\Omega^2 + 64\Gamma_2^2)/64\mu_1^2},$$

$$\phi = \arctan\left(-\frac{8\Gamma_2}{\Omega}\right). \tag{5}$$

Γ_2 in Eq. (5) is the dephasing rate that is defined as $\Gamma_2 = \Gamma_1/2 + \Gamma_\phi$.

The concurrence C of the stationary state ρ_∞ (hereafter called the stationary concurrence) and the fidelity F between ρ_∞ and the maximally entangled state ρ_m (hereafter called the stationary fidelity) are given by

$$C(\rho_\infty) = \max\left\{\frac{8\mu_1\sqrt{\Omega^2 + 64\Gamma_2^2} - 64\mu_1^2\Gamma_2/\Gamma_1}{128\mu_1^2\Gamma_2/\Gamma_1 + (\Omega^2 + 64\Gamma_2^2)}, 0\right\},$$

$$F(\rho_\infty) = \mathrm{tr}(\rho_m\rho_\infty) = \frac{4\mu_1\sqrt{\Omega^2 + 64\Gamma_2^2} - 32\mu_1^2\Gamma_2/\Gamma_1}{128\mu_1^2\Gamma_2/\Gamma_1 + (\Omega^2 + 64\Gamma_2^2)} + \frac{1}{2}. \tag{6}$$

The derivation of Eq. (6) is given in the Appendix.

Our calculations show that the stationary concurrence $C(\rho_\infty)$ and fidelity $F(\rho_\infty)$ are not affected by the interaction strength μ_2. Indeed, μ_2 induces a coherent superposition of the two eigenstates $|01\rangle$ and $|10\rangle$ (see Fig. 1). These two states always decay to the two-qubit ground state $|00\rangle$, when subject to independent relaxation and dephasing channels. Thus, μ_2 does not affect the stationary state ρ_∞. However, the interaction strength μ_1 induces a coherent superposition of the two eigenstates $|00\rangle$ and $|11\rangle$. Of course, $|00\rangle$ is already in the ground state, while the state $|11\rangle$ can be partially recovered from $|00\rangle$ by the coherent superposition caused by μ_1. Therefore, the stationary concurrence $C(\rho_\infty)$ and fidelity $F(\rho_\infty)$ only depend on μ_1.

As a remark, we should emphasize that the detuning between the single-qubit frequencies ω_{a1} and ω_{a2} should be large enough such that

$$|\omega_{a1} - \omega_{a2}| \sim |\omega_{a1} + \omega_{a2}|. \tag{7}$$

In fact, the effective two-qubit Hamiltonian in the interaction picture can be expressed as

$$H_A^{\mathrm{eff}} = \mu_1\{e^{i[(\omega_{a1}+\omega_{a2})t-\theta_1]}\sigma_+^{(1)}\sigma_+^{(2)} + \mathrm{H.c.}\} + \mu_2\{e^{i[(\omega_{a1}-\omega_{a2})t-\theta_2]}\sigma_+^{(1)}\sigma_-^{(2)} + \mathrm{H.c.}\}. \tag{8}$$

Under the condition in Eq. (7), the first and second terms in Eq. (8) are of the same order, so both terms should be kept. However, if the detuning between the single-qubit frequencies ω_{a1} and ω_{a2} is small enough, such that

$$|\omega_{a1} - \omega_{a2}| \ll |\omega_{a1} + \omega_{a2}|,$$

the nonrotating wave term

$$\exp i[(\omega_{a1} + \omega_{a2})t - \theta_1]\sigma_+^{(1)}\sigma_+^{(2)} + \mathrm{H.c.}$$

would be a fast-oscillating term which should be omitted, compared with the rotating-wave term. This implies that the μ_1 term in H_A^{eff} [Eq. (8)] would vanish, producing zero stationary entanglement, $C(\rho_\infty)=0$. In the following sections, we will use superconducting qubits as examples to show that the detuning condition in Eq. (7) can be satisfied by tuning the system parameters.

Of course, quantum systems acting as qubits usually have many energy levels (the two lowest energy levels are usually taken as the qubit). The condition in Eq. (7) means that two qubits have very different transition frequencies. Therefore, to make the two-level approximation valid for our proposal, the transition frequencies from the first excited state to the second excited state ΔE_1, ΔE_2 for each qubit system should be far larger than the qubit frequencies, i.e.,

$$\Delta E_1, \ \Delta E_2 \gg \omega_{a1}, \omega_{a2}, \tag{9}$$

so that the qubit with the highest frequency will not excite the higher energy levels of the qubit with the lower frequency. The condition in Eq. (9) can be satisfied. For example, when superconducting qubits work at their degeneracy points, the condition in Eq. (9) can indeed be satisfied (see, e.g., Figs. 1(a)–1(c) in Ref. [38(a)] and Figs. 2(a)–2(c) in Ref. [39], the two lowest energy states are far separated from the higher energy states at the flux degeneracy point $f = 0.5$). Thus, the two-level approximation is valid in these examples and can result in the Hamiltonian used for coupled superconducting qubits (e.g., in Refs. [8–10]).

Equation (6) shows that the maximum concurrence $C_{\max}$ and the maximum fidelity $F_{\max}$, where

$$C_{\max} = \frac{1}{4}\left(\sqrt{\frac{2\Gamma_1}{\Gamma_2} + 1} - 1\right),$$

$$F_{\max} = \frac{1}{8}\left(\sqrt{\frac{2\Gamma_1}{\Gamma_2} + 1} - 1\right) + \frac{1}{2}, \tag{10}$$

can be obtained when the parameters μ_1 and Ω satisfy

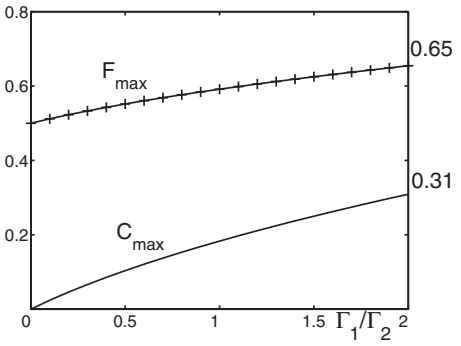

FIG. 2. Maximum concurrence $C_{\max}$ and maximum fidelity $F_{\max}$, versus the ratio Γ_1/Γ_2 of the relaxation rates, as given in Eq. (10). Note that $C_{\max}\to 0.31$ and $F_{\max}\to 0.65$ when $\Gamma_1/\Gamma_2\to 2$.

$$\mu_1 = \frac{\Gamma_1}{8}\frac{\sqrt{\Omega^2+64\Gamma_2^2}}{\sqrt{2\Gamma_1\Gamma_2+\Gamma_2^2}+\Gamma_2}. \tag{11}$$

The maximum concurrence $C_{\max}$ and fidelity $F_{\max}$, given in Eq. (10), are plotted in Fig. 2. This clearly shows that the concurrence $C_{\max}$ and fidelity $F_{\max}$ in Eq. (10) increase when the ratio

$$\frac{\Gamma_1}{\Gamma_2} = \frac{\Gamma_1}{\Gamma_1/2+\Gamma_\phi} \tag{12}$$

increases, and the highest concurrence and fidelity

$$C_{\max}\to\frac{\sqrt{5}-1}{4}\approx 0.31, \tag{13}$$

$$F_{\max}\to\frac{\sqrt{5}+3}{8}\approx 0.65 \tag{14}$$

can be obtained when $\Gamma_2\to\Gamma_1/2$, i.e., $\Gamma_\phi\to 0$.

The obtained maximum concurrence $C_{\max}$ may not be high enough to be used for demanding tasks in quantum information processing. However, there are two possible ways to increase the stationary entanglement. First, the ratio Γ_1/Γ_2 in Eq. (12) can approach the optimal value 2 for certain systems. For example, if the superconducting charge or flux qubits are at their degenerate points [1–3], the optimal value 2 might be obtained. In this case, the optimal concurrence and fidelity can be obtained, as shown in Eqs. (13) and (14).

Second, Eq. (10) shows that the maximum fidelity $F_{\max}$ between the stationary state ρ_∞ and the maximally entangled state ρ_m is always larger than 0.5, which makes it possible to introduce additional entanglement purification process to increase the proportion of the maximally entangled state ρ_m. Even if the concurrence and fidelity reach the optimal values, as in Eqs. (13) and (14), we can, in principle, further increase the stationary entanglement by using purification strategies, e.g., as in Refs. [40,41].

B. Weak interaction regime: $\mu_i \ll 10^{-1}(\omega_{a1}+\omega_{a2})$

The results obtained in Sec. II A cannot be efficiently applied to the case when $\mu_1,\mu_2\ll 10^{-1}\ \Omega$ (e.g., when μ_1,μ_2 are 2 orders of magnitude smaller than Ω). In fact, optimal condition (11) shows that we can obtain the maximum concurrence $C_{\max}$ and fidelity $F_{\max}$ only when

$$\mu_1 = \frac{\Gamma_1}{8}\frac{\sqrt{\Omega^2+64\Gamma_2^2}}{\sqrt{2\Gamma_1\Gamma_2+\Gamma_2^2}+\Gamma_2} \geq \frac{\Gamma_1}{8(\sqrt{5}+1)\Gamma_2}\Omega.$$

Thus, if $\mu_1\ll 10^{-1}\ \Omega$, then, optimally, the ratio Γ_1/Γ_2 should be very small. In this case, from Eq. (6), the obtained maximum stationary concurrence $C_{\max}$ will be extremely small. Alternatively, in order to avoid this problem, a time-dependent interaction between qubits should be introduced.

If the phase θ_1 in Eq. (1) can be tuned to be

$$\theta_1 = \Omega t+\phi_0 = (\omega_{a1}+\omega_{a2})t+\phi_0, \tag{15}$$

then the obtained long-time state ρ_∞ will be a time-dependent state

$$\rho_\infty(t) = \frac{\mu_1\Gamma_1}{2\mu_1^2+\Gamma_1\Gamma_2}\tilde{\rho}_m(t)+\left(1-\frac{\mu_1\Gamma_1}{2\mu_1^2+\Gamma_1\Gamma_2}\right)\tilde{\rho}_s$$

as a convex combination of a time-dependent maximally entangled state

$$\tilde{\rho}_m(t) = \frac{1}{2}\begin{pmatrix} 1 & & & e^{-i(\Omega t+\phi_0-\pi/2)} \\ & 0 & & \\ & & 0 & \\ e^{i(\Omega t+\phi_0-\pi/2)} & & & 1 \end{pmatrix}$$

and a time-independent diagonal separable state $\tilde{\rho}_s$:

$$\tilde{\rho}_s = \begin{pmatrix} 1-3\tilde{\beta} & & & \\ & \tilde{\beta} & & \\ & & \tilde{\beta} & \\ & & & \tilde{\beta} \end{pmatrix},$$

where

$$\tilde{\beta} = \frac{1}{8}\left(1-\sqrt{1-\frac{8\Gamma_2}{\Gamma_1}\left(\frac{\mu_1\Gamma_1}{2\mu_1^2+\Gamma_1\Gamma_2}\right)^2}\right).$$

The corresponding stationary concurrence and fidelity can now be expressed as

$$C(\rho_\infty) = \max\left\{\frac{\mu_1(\Gamma_1-\mu_1)}{2\mu_1^2+\Gamma_2\Gamma_1},0\right\},$$

$$F(\rho_\infty) = \frac{\mu_1(\Gamma_1-\mu_1)}{4\mu_1^2+2\Gamma_1\Gamma_2}+\frac{1}{2}. \tag{16}$$

The time-dependent phase θ_1 given in Eq. (15) induces a time-dependent coupling between qubits, which can be realized by applying an external time-dependent field (see Sec. V for a possible realization of such a coupling).

It should be pointed out that we do not need to introduce the detuning condition (7) in this case, because the fast-oscillating frequency of the nonrotating wave term "$e^{-i\theta_1}\sigma_+^{(1)}\sigma_+^{(2)}+\text{H.c.}$" can be offset by the time-dependent phase θ_1 in Eq. (15). In fact, in the interaction picture, the

two-qubit effective Hamiltonian can be written as

$$H_A^{\text{eff}} = \mu_2\{e^{i[(\omega_{a1}-\omega_{a2})t-\theta_2]}\sigma_+^{(1)}\sigma_-^{(2)} + \text{H.c.}\} + \mu_1(e^{-i\phi_0}\sigma_+^{(1)}\sigma_+^{(2)} + \text{H.c.}),$$

where the term "$e^{-i\phi_0}\sigma_+^{(1)}\sigma_+^{(2)}$+H.c." would not be a high-frequency term, and thus would contribute.

The condition that the nonrotating wave term is kept in H_A^{eff} above is that the frequency of the time-dependent modulation coupling the two qubits matches the sum of the two frequencies of the two qubits. Similar to the time-independent case in Sec. II A, this modulation might excite the high-energy levels of the quantum systems acting as qubits. Therefore, in this case, the two-level approximation requires that the transition frequencies from the first excited state to the second excited states ΔE_1, ΔE_2 should satisfy

$$\Delta E_1, \Delta E_2 \gg \omega_{a1} + \omega_{a2}. \tag{17}$$

This assumption is valid when the superconducting qubits discussed below are at their degeneracy points.

For the same reason discussed in Sec. II A, the stationary concurrence $C(\rho_\infty)$ and fidelity $F(\rho_\infty)$ are not affected by the interaction strength μ_2. The proof of Eq. (16) is similar to the proof of Eq. (6). From Eq. (16), the maximum stationary concurrence and fidelity

$$C_{\max} = \frac{1}{4}\left(\sqrt{\frac{2\Gamma_1}{\Gamma_2}+1}-1\right),$$

$$F_{\max} = \frac{1}{8}\left(\sqrt{\frac{2\Gamma_1}{\Gamma_2}+1}-1\right)+\frac{1}{2} \tag{18}$$

can be obtained when

$$\mu_1 = \frac{\Gamma_1\Gamma_2}{\sqrt{2\Gamma_1\Gamma_2+\Gamma_2^2}+\Gamma_2}. \tag{19}$$

A higher stationary concurrence and fidelity can be obtained, as in the strong interaction regime, by increasing the ratio Γ_1/Γ_2. Below, we apply the above results to several superconducting circuits and discuss how their parameters can be varied so that the stationary concurrence and fidelity can be maxima.

C. Additional discussions of our model

In Secs. II A and II B, we consider the ideal case when the relaxation rates and the dephasing rates of the two qubits are equal. In practice, the two qubits may not have identical decoherence rates, especially when the single-qubit frequencies satisfy condition (7). However, additional calculations show that different decoherence rates do not greatly affect our main results. In order to investigate the influence of nonidentical decoherence rates on the optimal concurrence given in Eq. (13), let us now assume that the two qubits are both at the degeneracy points, i.e., $\Gamma_1^{(i)}=2\Gamma_2^{(i)}$, $i=1,2$, for the ith qubit, and the coupling strength μ_1 is chosen to be

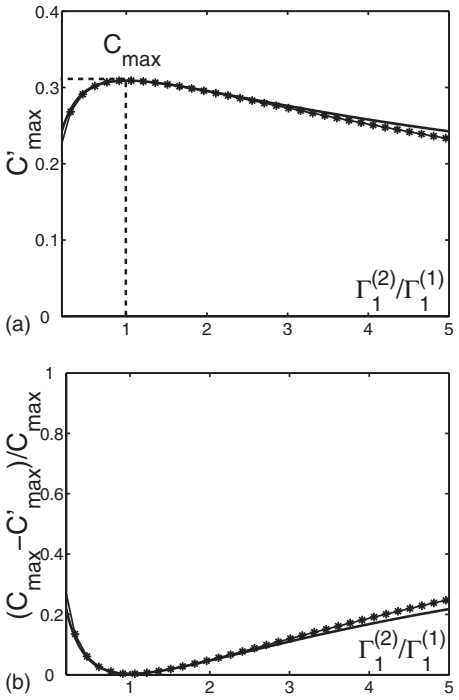

FIG. 3. Influence of nonidentical decoherence rates for two qubits on the maximum concurrence. (a) The maximum concurrence $C'_{\max}$ versus the ratio between the relaxation rates of the two qubits $\Gamma_1^{(2)}/\Gamma_1^{(1)}$; (b) the ratio $(C_{\max}-C'_{\max})/C_{\max}$, where $C_{\max}$ is the ideal maximum concurrence given in Eq. (13). The solid lines and the solid lines with asterisks represent, respectively, the cases when the qubits interact strongly and weakly.

$$\mu_1 = \frac{\bar{\Gamma}_1}{8}\frac{\sqrt{\Omega^2+64\bar{\Gamma}_2^2}}{\sqrt{2\bar{\Gamma}_1\bar{\Gamma}_2+\bar{\Gamma}_2^2}+\bar{\Gamma}_2}$$

for the strong interaction case, and

$$\mu_1 = \frac{\bar{\Gamma}_1\bar{\Gamma}_2}{\sqrt{2\bar{\Gamma}_1\bar{\Gamma}_2+\bar{\Gamma}_2^2}+\bar{\Gamma}_2}$$

for the weak interaction case, where $\bar{\Gamma}_1=(\Gamma_1^{(1)}+\Gamma_1^{(2)})/2$ and $\bar{\Gamma}_2=(\Gamma_2^{(1)}+\Gamma_2^{(2)})/2$ are, respectively, the average relaxation and dephasing rates of the two qubits. As shown in Fig. 3, when the ratio between the relaxation rates of the two qubits is less than 5, i.e., $0.2\leq\Gamma_1^{(1)}/\Gamma_1^{(2)}\leq 5$, the difference between the concurrence $C'_{\max}$ obtained in this case and the ideal maximum concurrence $C_{\max}$ given in Eq. (13) is about 20% of $C_{\max}$. The above analysis shows that different decoherence rates do not greatly affect the optimal concurrence. Thus, in the following discussions we only consider the ideal case when the decoherence rates of the two qubits are identical.

Additionally, in Secs. II A and II B, we only consider independent decoherence channel. In general, the decoherence channel of the two-qubit system may be a mixture of independent and collective decoherence channels. If the two-qubit interaction Hamiltonian does not include the nonrotating wave term $\sigma_+^{(1)}\sigma_+^{(2)}$+H.c., i.e., $\mu_1=0$ in Eq. (1), it can be verified by the approach introduced in the Appendix that the

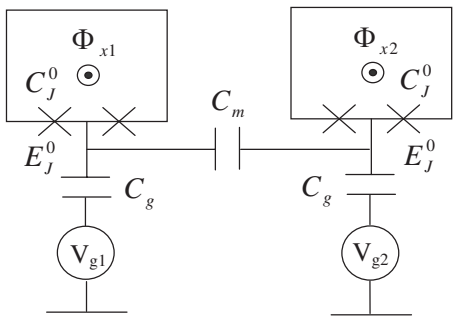

FIG. 4. Schematic diagram of two capacitively coupled CPBs.

stationary state of the two-qubit system under a mixture of independent and collective decoherence channels is the same as that under the pure independent decoherence channels discussed in Secs. II A and II B. It is different when we add the nonrotating wave term $\sigma_+^{(1)}\sigma_+^{(2)}+\text{H.c.}$. For example, the stationary concurrence in this case may depend on the initial state of the two-qubit system. However, under this condition, it is difficult to obtain an explicit expression of the stationary concurrence like those in Eqs. (6) and (16). Thus, the entanglement protection for this general situation is still an open problem.

Furthermore, we only consider the relaxation and pure-dephasing rates of the qubits. Apart from these exponential damping terms, there exist other sources of decoherence which cannot be expressed like this, especially those from the low-frequency noises. For example, the phase noises from the charge, critical-current, and flux $1/f$ fluctuations induce complex damping terms, which can be expressed as logarithm terms or the products of slowly varying logarithm terms and fast damping t^2 terms, and cannot be understood as rates (see, e.g., Eqs. (32) and (33) in Ref. [35]). However, as shown in Ref. [35], this kind of noises can be significantly reduced by spin echo or Rabi sequences. The effective decoherence rate γ_ϕ induced by $1/f$ noises can be reduced to be in the ms^{-1} regime by these approaches. For this reason, we can omit this kind of noises in our discussions.

III. DIRECT COUPLING BETWEEN SUPERCONDUCTING QUBITS

A. Two capacitively coupled charge qubits

Let us first study the superconducting circuit shown in Fig. 4, where two single Cooper pair boxes (CPBs) are connected via a small capacitor [5,6]. The Hamiltonian of the total system can be

$$H_A=\sum_{j=1}^{2}[4E_C(\hat{n}_j-n_{gj})^2-E_J(\Phi_{xj})\cos\hat{\phi}_j]+4J\hat{n}_1\hat{n}_2, \tag{20}$$

where $\hat{\phi}_j$ is a phase operator denoting the phase drop across the jth CPB; $\hat{n}_j=-i\partial/(\partial\hat{\phi}_j)$, which represents the number of Cooper pairs on the island electrode, is the conjugate operator of $\hat{\phi}_j$. The reduced charge number n_{gj}, in units of the Cooper pairs $(2e)$, can be given by $n_{gj}=-C_gV_{gj}/2e$, where the parameters C_g and V_{gj} are the gate capacitance and gate voltage of the jth CPB. The Josephson energy $E_J(\Phi_{xj})$ of the jth dc superconducting quantum interference device (SQUID) is

$$E_J(\Phi_{xj})=2E_J^0\cos\left(\pi\frac{\Phi_{xj}}{\Phi_0}\right),$$

where E_J^0 represents the Josephson energy of a single Josephson junction [42]; Φ_{xj} denotes the external flux piercing the SQUID loop of the jth CPB; and Φ_0 is the flux quantum. The coupling constant J between two CPBs is

$$J=\frac{e^2C_m}{(C_g+2C_J^0)^2-C_m^2},$$

where C_J^0 and C_m are the capacitance of a single Josephson junction and the coupling capacitance between two CPBs. $E_C=e^2/2(C_g+2C_J^0)$ is the single-electron charging energy of a single CPB. For simplicity, we assume that E_C and E_J^0 are the same for the two CPBs.

Near $n_{gj}=0.5$, which is called the charge degenerate point, the two energy levels of the jth CPB corresponding to $n_j=0,1$ are close to each other and far separated from other high-energy levels. In this case, a single CPB can be approximately considered as a two-level system. In the charge basis, the Hamiltonian H_A in Eq. (20) can be written as [2]

$$H_A=\sum_{j=1}^{2}\left[-\frac{1}{2}E_C(n_{gj})\tilde{\sigma}_z^{(j)}-\frac{1}{2}E_J(\Phi_{xj})\tilde{\sigma}_x^{(j)}\right]+J\tilde{\sigma}_z^{(1)}\tilde{\sigma}_z^{(2)}, \tag{21}$$

where $E_C(n_{gj})=4E_C(1-2n_{gj})$ and the Pauli operators are defined as

$$\tilde{\sigma}_x^{(j)}=|0\rangle_{jj}\langle 1|+|1\rangle_{jj}\langle 0|,$$

$$\tilde{\sigma}_z^{(j)}=|0\rangle_{jj}\langle 0|-|1\rangle_{jj}\langle 1|.$$

Here, $|0\rangle_j$ and $|1\rangle_j$ are the charge states with the Cooper pair numbers $n_j=0,1$, respectively.

Rewriting Eq. (21) using the eigenstates of the single-qubit Hamiltonian, we have

$$H_A=\sum_{j=1}^{2}\frac{\omega_{aj}}{2}\sigma_z^{(j)}+J\prod_{j=1}^{2}\left(\frac{E_{Jj}}{\omega_{aj}}\sigma_x^{(j)}-\frac{E_{Cj}}{\omega_{aj}}\sigma_z^{(j)}\right),$$

with $\omega_{aj}=(E_{Cj}^2+E_{Jj}^2)^{1/2}$, $E_{Cj}=E_C(n_{gj})$, and $E_{Jj}=E_J(\Phi_{xj})$. The new Pauli operators $\sigma_x^{(j)}$ and $\sigma_z^{(j)}$ are defined by the eigenstates $|+\rangle_j$ and $|-\rangle_j$ of the jth qubit as

$$\sigma_x^{(j)}=|+\rangle_{jj}\langle -|+|-\rangle_{jj}\langle +|,$$

$$\sigma_z^{(j)}=|+\rangle_{jj}\langle +|-|-\rangle_{jj}\langle -|,$$

where

$$|+\rangle_j=\cos\theta_j|0\rangle_j-\sin\theta_j|1\rangle_j,$$

$$|-\rangle_j=\sin\theta_j|0\rangle_j+\cos\theta_j|1\rangle_j.$$

Here, $\theta_j=[\arctan(-E_{Jj}/E_{Cj})]/2$.

Now, the two-qubit state $\rho(t)$ evolves following the master equation:

$$\dot{\rho} = -i[H_A,\rho] + \sum_{j=1}^{2} \Gamma_1 \mathcal{D}[\sigma_-^{(j)}]\rho + \sum_{j=1}^{2} 2\Gamma_\phi \mathcal{D}[\sigma_z^{(j)}]\rho.$$

Let us now assume that the two qubits are both in the charge degenerate point $n_{gj}=0.5$ with $E_{Cj}=0$, so that the dephasing effects can be minimized. In this case, we have $\Gamma_\phi=0$, which means that $\Gamma_2=\Gamma_1/2+\Gamma_\phi=\Gamma_1/2$. Further, from $E_{Cj}=0$, we have

$$H_A = \sum_{j=1}^{2} \frac{E_J(\Phi_{xj})}{2}\sigma_z^{(j)} + J\sigma_x^{(1)}\sigma_x^{(2)} = \sum_{j=1}^{2} \frac{E_J(\Phi_{xj})}{2}\sigma_z^{(j)} + \frac{J}{4}(\sigma_+^{(1)}\sigma_+^{(2)} + \sigma_-^{(1)}\sigma_-^{(2)}) + \frac{J}{4}(\sigma_+^{(1)}\sigma_-^{(2)} + \sigma_-^{(1)}\sigma_+^{(2)}).$$

In some experiments (e.g., [5]), the coupling strength J is of the same order of

$$\Omega = 2E_J^0 \sum_{j=1}^{2} \cos\left(\pi \frac{\Phi_{xj}}{\Phi_0}\right),$$

where $J \approx 4$ GHz, $E_J^0 \approx 10$ GHz and the decoherence rates [43] Γ_1, Γ_2 are of the order of 10–100 MHz $\ll J, \Omega$.

By substituting Ω and $\mu_1=J/4$ into optimal condition (11), then, in the limit $\Omega \gg \Gamma_1, \Gamma_2$, the maximum concurrence $C_{\max} \approx 0.31$ and fidelity $F_{\max} \approx 0.65$, as in Eqs. (13) and (14), can be obtained, if the fluxes Φ_{x1} and Φ_{x2} are tuned such that

$$\cos\left(\pi \frac{\Phi_{x1}}{\Phi_0}\right) + \cos\left(\pi \frac{\Phi_{x2}}{\Phi_0}\right) \approx \frac{\sqrt{5}+1}{2}\frac{J}{E_J^0}. \tag{22}$$

Furthermore, detuning condition (7) requires that Φ_{x1} and Φ_{x2} should be tuned such that

$$0 < \pi \frac{\Phi_{x1}}{\Phi_0} \ll \pi \frac{\Phi_{x2}}{\Phi_0} < \frac{\pi}{2},$$

or

$$0 < \pi \frac{\Phi_{x2}}{\Phi_0} \ll \pi \frac{\Phi_{x1}}{\Phi_0} < \frac{\pi}{2}. \tag{23}$$

The above two conditions (22) and (23) can be satisfied in experiments.

B. Two inductively coupled flux qubits

Let us now consider a superconducting circuit, as shown in Fig. 5, where two flux qubits are coupled through their mutual inductance. Here, we modify the design used in the experimental device in Ref. [9]. Namely, the small junction of each three-junction flux qubit is replaced by a dc SQUID, from which we can adjust the tunneling amplitude between the left and right wells (see Fig. 6) of each single flux qubit.

Near the flux degenerate point $\Phi_j \approx \Phi_0/2$, with the external flux Φ_j piercing the superconducting loop of the jth qubit, each flux qubit behaves as a two-level system. The total Hamiltonian of the two-qubit system can be expressed as [9]

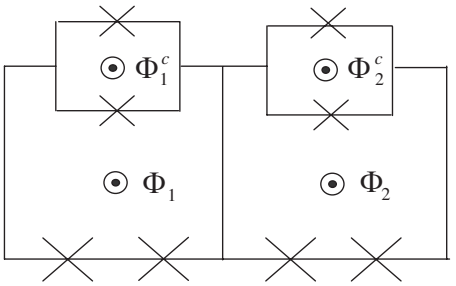

FIG. 5. Schematic diagram of two flux qubits coupled via their mutual inductance.

$$H_A = -\frac{1}{2}\sum_{j=1}^{2} [\epsilon(\Phi_j)\tilde{\sigma}_z^{(j)} + \Delta(\Phi_j^c)\tilde{\sigma}_x^{(j)}] + J\tilde{\sigma}_z^{(1)}\tilde{\sigma}_z^{(2)}, \tag{24}$$

where

$$\tilde{\sigma}_x^{(j)} = |L_j\rangle\langle R_j| + |R_j\rangle\langle L_j|,$$

$$\tilde{\sigma}_z^{(j)} = |L_j\rangle\langle L_j| - |R_j\rangle\langle R_j|,$$

and $|L_j\rangle, |R_j\rangle$ are the two lowest energy states in the left and right wells of the jth flux qubit (see Fig. 6). The parameter $\epsilon(\Phi_j)$ denotes the energy difference between $|L_j\rangle$ and $|R_j\rangle$ which can be expressed as

$$\epsilon(\Phi_j) = 2I_{pj}\left(\Phi_j - \frac{1}{2}\Phi_0\right),$$

where I_{pj} is the circulating current in the loop of the jth qubit. The tunneling amplitude $\Delta(\Phi_j^c)$ between the two wells is tunable by varying the magnetic flux Φ_j^c piercing the jth dc-SQUID. In the limit

$$0 < \frac{2\pi L_j I_c(\Phi_j^c)}{\Phi_0} - 1 \ll 1,$$

$\Delta(\Phi_j^c)$ can be approximately expressed as [20]

$$\Delta(\Phi_j^c) \approx \frac{3\Phi_0^2}{8\pi^2 L_j}\left(1 - \frac{\Phi_0}{2\pi L_j I_c(\Phi_j^c)}\right)^2,$$

where L_j is the self-inductance of the superconducting loop of the jth flux qubit, and

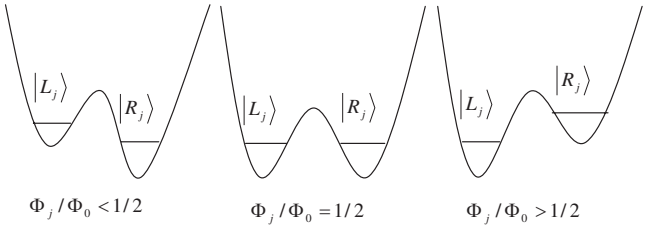

FIG. 6. Schematic diagram of the double-well potential of the jth flux qubit with the two lowest-energy states for $\Phi_j < \Phi_0/2$, $\Phi_j = \Phi_0/2$, and $\Phi_j > \Phi_0/2$.

$$I_c(\Phi_j^c) = 2I_0 \left| \cos\left(\frac{\pi \Phi_j^c}{\Phi_0} \right) \right|$$

is the tunable critical current of the jth dc-SQUID, with I_0 being the maximum critical current. The coupling strength J between the two flux qubits is

$$J = MI_{p1}I_{p2},$$

with the mutual inductance M between the two flux qubits.

Let us now assume that $\Phi_j = \Phi_0/2$, then the two-qubit Hamiltonian in Eq. (24) can be further simplified to

$$H_A = \frac{1}{2}\sum_{j=1}^{2} \Delta(\Phi_j^c)\sigma_z^{(j)} + \frac{J}{4}(\sigma_+^{(1)}\sigma_+^{(2)} + \sigma_-^{(1)}\sigma_-^{(2)}) + \frac{J}{4}(\sigma_+^{(1)}\sigma_-^{(2)} + \sigma_-^{(1)}\sigma_+^{(2)}),$$

where

$$\sigma_x^{(j)} = |+\rangle_{jj}\langle -| + |-\rangle_{jj}\langle +|,$$

$$\sigma_z^{(j)} = |+\rangle_{jj}\langle +| - |-\rangle_{jj}\langle -|,$$

and

$$|+\rangle_j = \frac{\sqrt{2}}{2}\{|L_j\rangle - |R_j\rangle\},$$

$$|-\rangle_j = \frac{\sqrt{2}}{2}\{|L_j\rangle + |R_j\rangle\}.$$

The decoherence process can be described by the master Eq. (2) under the Born-Markov approximation. At the degenerate point $(\Phi_j = \Phi_0/2; j = 1,2)$, we have $\Gamma_\phi = 0$, which means that $\Gamma_2 = (\Gamma_1/2) + \Gamma_\phi = \Gamma_1/2$.

By substituting

$$\Omega = \Delta(\Phi_1^c) + \Delta(\Phi_2^c), \quad \mu_1 = \frac{J}{4}$$

into optimal condition (11), then, in the limit $\Delta(\Phi_j^c)$, $J \gg \Gamma_1, \Gamma_2$, the maximum concurrence $C_{\max} \approx 0.31$ and fidelity $F_{\max} \approx 0.65$ can be obtained when

$$\Delta(\Phi_1^c) + \Delta(\Phi_2^c) \approx (\sqrt{5}+1)J. \tag{25}$$

Furthermore, detuning condition (7) requires that $\Delta(\Phi_j^c)$ should be tuned such that

$$|\Delta(\Phi_1^c)| \ll |\Delta(\Phi_2^c)| \text{ or } |\Delta(\Phi_2^c)| \ll |\Delta(\Phi_1^c)|. \tag{26}$$

In experiments (e.g., in Ref. [9]), $\Delta(\Phi_j^c)$ and J are of the same order (~ 1 GHz) that are far larger than the decoherence rates $\Gamma_1, \Gamma_2 \sim 1-10$ MHz (see, e.g., [44]). Thus, conditions (25) and (26) could be realized in experiments.

IV. TUNABLE COUPLING BETWEEN SUPERCONDUCTING QUBITS: STRONG-INTERACTION REGIME

There are two ways to tune the system parameters to achieve optimal condition (11). One way is by tuning the sum of the single-qubit oscillating frequencies Ω, which was used in Sec. III. In this section, we study another way to achieve optimal condition (11) by tuning the coupling strength μ_1 between the two qubits.

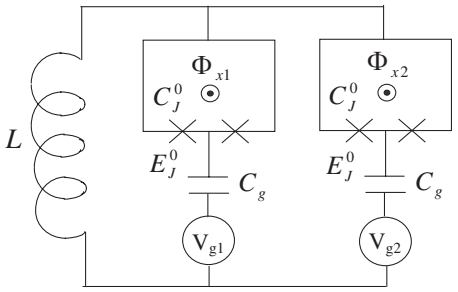

FIG. 7. Schematic diagram of two charge qubits coupled via an LC oscillator.

A. Variable coupling between two charge qubits

Many strategies have been proposed to obtain a controllable coupling between qubits (see, e.g., [16,17,20–27]). Let us first study the superconducting circuit shown in Fig. 7, where two CPBs are coupled via an LC oscillator. This strategy was first proposed in Ref. [16] and also investigated by other researchers (e.g., in Ref. [45]). In the charge degenerate point, the two-qubit Hamiltonian in Refs. [1,16] is

$$H_A = -\sum_{j=1}^{2} \frac{1}{2} E_J(\Phi_{xj})\tilde{\sigma}_x^{(j)} - E_{\text{int}}\tilde{\sigma}_y^{(1)}\tilde{\sigma}_y^{(2)}, \tag{27}$$

with $E_{\text{int}} = E_J(\Phi_{x1})E_J(\Phi_{x2})/E_L$ and $E_J(\Phi_{xj}) = 2E_J^0 \cos(\pi\Phi_{xj}/\Phi_0)$. Here

$$\tilde{\sigma}_x^{(j)} = |0\rangle_{jj}\langle 1| + |1\rangle_{jj}\langle 0|,$$

$$\tilde{\sigma}_y^{(j)} = -i|0\rangle_{jj}\langle 1| + i|1\rangle_{jj}\langle 0|,$$

and $|0\rangle_j, |1\rangle_j$ are the two charge states of the jth CPB. The quantity E_L in the expression above for the coupling strength E_{int} can be written as

$$E_L = \left(\frac{2C_J^0}{C_{qb}} \right)^2 \frac{\Phi_0^2}{\pi^2 L},$$

where $C_{qb} = 2C_J^0 C_g [2C_J^0 + C_g]^{-1}$ is the capacitance of a single CPB in the external circuit, and L is the inductance of the coupling current-biased inductor.

Rewriting Eq. (27) under the eigenstates of the single-qubit Hamiltonian, we have

$$H_A = \sum_{j=1}^{2} \frac{E_J(\Phi_{xj})}{2}\sigma_z^{(j)} + \frac{E_{\text{int}}}{4}(\sigma_+^{(1)}\sigma_+^{(2)} + \sigma_-^{(1)}\sigma_-^{(2)}) - \frac{E_{\text{int}}}{4}(\sigma_+^{(1)}\sigma_-^{(2)} + \sigma_-^{(1)}\sigma_+^{(2)}),$$

where

$$\sigma_z^{(j)} = |+\rangle_{jj}\langle +| - |-\rangle_{jj}\langle -| = -\tilde{\sigma}_x^{(j)},$$

$$\sigma_y^{(j)} = -i|+\rangle_{jj}\langle -| + i|-\rangle_{jj}\langle +| = \tilde{\sigma}_y^{(j)},$$

and

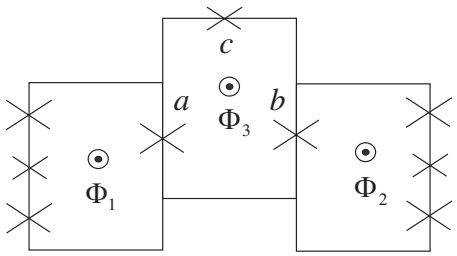

FIG. 8. Schematic diagram of two three-junction flux qubits coupled via an auxiliary flux qubit.

$$|+\rangle_j = \frac{1}{\sqrt{2}}\{|0\rangle_j - |1\rangle_j\},$$

$$|-\rangle_j = \frac{1}{\sqrt{2}}\{|0\rangle_j + |1\rangle_j\}.$$

Since $\Gamma_2=\Gamma_1/2$ at the charge degenerate point, then, replacing Ω and μ_1 in Eq. (11) by $\Sigma_j E_J(\Phi_{xj})$ and $E_{\rm int}/4$, the maximum concurrence $C_{\max}\approx 0.31$ and fidelity $F_{\max}\approx 0.65$ can be obtained when the external fluxes Φ_{x1} and Φ_{x2} are tuned such that

$$\cos\left(\pi\frac{\Phi_{x1}}{\Phi_0}\right)+\cos\left(\pi\frac{\Phi_{x2}}{\Phi_0}\right)\approx\frac{2}{\sqrt{5}+1}\frac{E_L}{E_J^0},$$

when these conditions hold: $E_L, E_J^0 \gg \Gamma_1, \Gamma_2$. Furthermore, detuning condition (7) requires that Φ_{x1}, Φ_{x2} should satisfy condition (23).

B. Variable coupling between two flux qubits

Our strategy can also be applied to flux qubits with controllable coupling. Here, let us consider a superconducting circuit design as in Ref. [21] (see Fig. 8), where two three-junction flux qubits (qubits 1 and 2) are coupled via an auxiliary three-junction flux qubit (qubit 3). This middle flux qubit (qubit 3), acting as a coupler, is connected to qubits 1 and 2 by sharing junctions a and b with the same Josephson energy E_J^0, while junction c is smaller than a and b, with Josephson energy $\alpha E_J^0, \alpha<1$. By adiabatically eliminating the degrees of freedom of the auxiliary flux qubit 3, the total Hamiltonian of the flux qubits 1 and 2 becomes [21]

$$H_A = -\frac{1}{2}\sum_{j=1}^{2}[\epsilon(\Phi_j)\tilde{\sigma}_z^{(j)}+\Delta_j\tilde{\sigma}_x^{(j)}]+J(\Phi_3)\tilde{\sigma}_z^{(1)}\tilde{\sigma}_z^{(2)},$$

where $\epsilon(\Phi_j)$, $\Delta_j, j=1,2$, $\tilde{\sigma}_z^{(j)}$, and $\tilde{\sigma}_x^{(j)}$ have the same meaning as in Sec. III B. When $\alpha \ll 1$, the coupling strength $J(\Phi_3)$ between the two flux qubits 1 and 2 becomes [21]

$$J(\Phi_3)\approx\frac{\alpha I_{p1}I_{p2}}{4e^2E_J^0}\cos\left(2\pi\frac{\Phi_3}{\Phi_0}\right)\equiv J_0\cos\left(2\pi\frac{\Phi_3}{\Phi_0}\right). \quad (28)$$

From Eq. (28), the coupling strength $J(\Phi_3)$ is tunable by varying the flux Φ_3 piercing the superconducting loop of the auxiliary qubit 3.

At the flux degenerate point, i.e., $\Phi_j=\Phi_0/2$ for both qubits, and using the eigenstates of the single-qubit Hamiltonian, we have

$$H_A=\frac{1}{2}\sum_{j=1}^{2}\Delta_j\sigma_z^{(j)}+J(\Phi_3)\sigma_x^{(1)}\sigma_x^{(2)}=\frac{1}{2}\sum_{j=1}^{2}\Delta_j\sigma_z^{(j)}$$
$$+\frac{J(\Phi_3)}{4}(\sigma_+^{(1)}\sigma_+^{(2)}+\sigma_-^{(1)}\sigma_-^{(2)})+\frac{J(\Phi_3)}{4}(\sigma_+^{(1)}\sigma_-^{(2)}+\sigma_-^{(1)}\sigma_+^{(2)}).$$

Since the two flux qubits are at their flux degenerate points, then, replacing Ω and μ_1 in Eq. (11) by $\Delta_1+\Delta_2$ and $J(\Phi_3)/4$, the maximum stationary concurrence $C_{\max}\approx 0.31$ and fidelity $F_{\max}\approx 0.65$ can be obtained when $J(\Phi_3)\approx(\Delta_1+\Delta_2)/(\sqrt{5}+1)$, i.e.,

$$\cos\left(2\pi\frac{\Phi_3}{\Phi_0}\right)\approx\frac{(\Delta_1+\Delta_2)}{(\sqrt{5}+1)J_0},$$

when these conditions hold: $\Delta_1, \Delta_2, J_0 \gg \Gamma_1, \Gamma_2$.

From the experiment [21], where Δ_1, Δ_2, and J_0 are of the same order ($\sim$1 GHz) and far larger than Γ_1, Γ_2 ($\sim$1–10 MHz), the above optimal condition could be satisfied by varying the magnetic flux Φ_3 through the middle superconducting loop.

Furthermore, in order to satisfy detuning condition (7), the tunneling amplitude Δ_j of the flux qubits should satisfy

$$|\Delta_1| \ll |\Delta_2| \quad \text{or} \quad |\Delta_2| \ll |\Delta_1|.$$

This can be realized by replacing the small junctions of the two flux qubits (on the left and right of Fig. 8) by dc-SQUIDs, to introduce extra control parameters, just like what we have done in Fig. 6.

V. TUNABLE COUPLING BETWEEN SUPERCONDUCTING QUBITS: WEAK INTERACTION REGIME

In this section, we study how to prepare entangled states in superconducting circuits where two charge qubits are coupled to a one-dimensional transmission line resonator. Since the interaction strength (10–100 MHz) between the two charge qubits coupled via the resonator is far smaller than the single-qubit oscillating frequency (5–15 GHz), then we are now considering the weak-interaction regime. From the analysis in Sec. II B, in order to prepare entangled states in this case, the following time-dependent interaction Hamiltonian should be introduced:

$$H_{\rm int}=\mu_1(e^{-i(\Omega t+\phi_0)}\sigma_+^{(1)}\sigma_+^{(2)}+e^{i(\Omega t+\phi_0)}\sigma_-^{(1)}\sigma_-^{(2)}).$$

The main idea in this section is the following: borrowing strategies that produce controllable squeezed fields in optical cavities (see, e.g., [46]), an auxiliary flux qubit circuit is introduced to squeeze the oscillating mode in the resonator (see Fig. 9). The auxiliary flux qubit circuit in fact acts like a Δ-shaped three-level atom which is further driven by a classical field. By adiabatically eliminating the degrees of freedom of the auxiliary flux qubit circuit, one can obtain a controllable squeezed field in the resonator where the squeezed

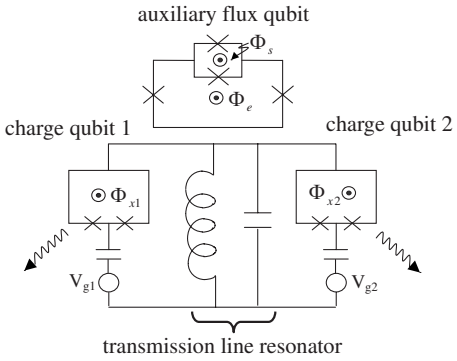

FIG. 9. Schematic diagram of our proposal for producing quantum entanglement in two charge qubits coupled to a resonator.

coefficient is tunable by changing the coupling strength between the classical driving field and the auxiliary flux qubit. With the help of the controllable squeezed field in the resonator, one can continuously adjust the stationary entanglement between the two qubits.

A. Controllable squeezed electric field in a transmission line resonator

We first show how to obtain a controllable squeezed electric field [47–50] in the resonator by using a theoretical proposal of realizing squeezed states in cavities [46]. The auxiliary flux qubit circuit in our proposal (shown in Fig. 9) acts as a three-level system with Δ-type transition [38,39].

As depicted in Fig. 10, we are now considering a three-level system with a ground energy level $|g\rangle$, an intermediate energy level $|i\rangle$, and an excited energy level $|e\rangle$. Here, the transitions $|g\rangle \leftrightarrow |i\rangle$ and $|e\rangle \leftrightarrow |i\rangle$ are coupled dispersively to the quantized cavity mode in the resonator, with coupling strengths λ_g and λ_e. The transition $|g\rangle \leftrightarrow |e\rangle$ is coupled dispersively to a classical field with coupling strength λ_d and frequency $\tilde{\Omega}$. In the rotating-wave approximation, the total Hamiltonian of the three-level artificial atom and the resonator can be expressed as $H=H_0+V$, with

$$H_0 = \tilde{\omega}_c a^\dagger a - \tilde{\omega}_c |g\rangle\langle g| + \delta |i\rangle\langle i| + \tilde{\omega}_c |e\rangle\langle e|,$$

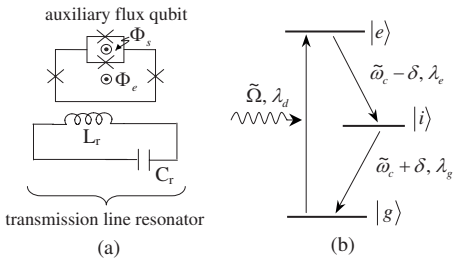

FIG. 10. Schematic diagrams for realizing a controllable squeezed electromagnetic field in a resonator coupled to an auxiliary flux qubit. (a) The auxiliary flux qubit and the transmission line resonator: the parameters in the auxiliary flux qubit are the same as those in Ref. [39]; by varying the flux Φ_s threading through the SQUID loop one can obtain a Δ-shaped three-level artificial atom. (b) Transition energy-level diagram of the Δ-shaped three-level artificial atom.

$$V = (\lambda_g a|i\rangle\langle g| + \text{H.c.}) + (\lambda_e a|e\rangle\langle i| + \text{H.c.}) + (\lambda_d |e\rangle\langle g| e^{-i\Omega t} + \text{H.c.}), \quad (29)$$

where H.c. means Hermitian conjugate; $\tilde{\omega}_c$ is the frequency of the resonator; δ is defined as a detuning from the energy levels $|e\rangle$ and $|g\rangle$ to the intermediate energy level $|i\rangle$.

Let us initially prepare the artificial atom in the intermediate level $|i\rangle$. With the help of the dispersive-detuning condition

$$\delta \gg |\lambda_g|, |\lambda_e|, |\tilde{\Omega} - 2\tilde{\omega}_c|,$$

one can obtain the following reduced Hamiltonian by adiabatically eliminating the degrees of freedom of the three-level artificial atom [46]:

$$H_c = \omega_c a^\dagger a + \xi(e^{-i(\tilde{\Omega}t+\tilde{\phi}_0)} a^{\dagger 2} + e^{i(\tilde{\Omega}t+\tilde{\phi}_0)} a^2), \quad (30)$$

where

$$\omega_c = \tilde{\omega}_c + \frac{2}{\delta}(|\lambda_g|^2 + |\lambda_e|^2)$$

is the effective frequency of the cavity mode; ξ and $\tilde{\phi}_0$ are *the effective amplitude and the initial phase of the squeezed field*. The relation between ξ and $\tilde{\phi}_0$ is given by

$$\xi \exp(i\tilde{\phi}_0) = \frac{2}{\delta^2} \lambda_d \lambda_g \lambda_e.$$

Notice that one can *continuously adjust* ξ by varying the coupling strength λ_d between the classical field and the three-level artificial atom.

B. Tunable coupling between qubits

In Fig. 9, let us now consider the interaction between the two charge qubits and the cavity field. After eliminating the degrees of freedom of the auxiliary three-level system, we can obtain the following total Hamiltonian of the charge qubits and the cavity field:

$$H = \xi(e^{-i(\tilde{\Omega}t+\tilde{\phi}_0)} a^{\dagger 2} + e^{i(\tilde{\Omega}t+\tilde{\phi}_0)} a^2) + \sum_{j=1}^{2} g(\eta_j - \cos\alpha_j \sigma_z^{(j)} + \sin\alpha_j \sigma_x^{(j)})(a^\dagger + a) + \frac{1}{2}\sum_{j=1}^{2} \omega_{aj} \sigma_z^{(j)} + \omega_c a^\dagger a, \quad (31)$$

where

$$\omega_{aj} = \sqrt{E_J^2(\Phi_{xj}) + E_C^2(n_{gj})}$$

has the same meaning with the corresponding quantity in Secs. III and IV; $g=-e(C_g/C_\Sigma)V_{\text{rms}}^0$ is the coupling strength between the resonator and a single qubit; C_Σ is the total capacitance of a qubit; $V_{\text{rms}}^0=\sqrt{\omega_c/2C_r}$ is the root mean square (rms) of the voltage across the LC circuit; C_r is the capacitance of the resonator; $\eta_j=1-2n_{gj}$; and the angle $\alpha_j = \arctan[E_J(\Phi_{xj})/E_C(1-2n_{gj})]$.

By using the rotating-wave approximation and assuming that $n_{gj}=1/2(j=1,2)$, the total Hamiltonian H in Eq. (31) can be rewritten as [36]

$$H_{JC} = \omega_c a^\dagger a + \sum_{j=1}^{2} \frac{E_J(\Phi_x)}{2} \sigma_z^{(j)} + \sum_{j=1}^{2} g(a^\dagger \sigma_-^{(j)} + a\sigma_+^{(j)})$$

$$+ \xi(e^{-i(\tilde{\Omega}t+\tilde{\phi}_0)} a^{\dagger 2} + e^{i(\tilde{\Omega}t+\tilde{\phi}_0)} a^2).$$

Here, to simplify our discussions, we have set $\Phi_{x1}=\Phi_{x2}=\Phi_x$.

We now assume that the qubits and the cavity field are in the dispersive regime, i.e.,

$$\Delta = [E_J(\Phi_x) - \omega_c] \sim 100 \text{ MHz} \gg |g| \sim 10 \text{ MHz}.$$

Thus, we can introduce the following unitary transformation to diagonalize the Hamiltonian H_{JC}:

$$U = \exp\left[\frac{g}{\Delta}\sum_{j=1}^{2}(a\sigma_+^{(j)} - a^\dagger \sigma_-^{(j)})\right].$$

Up to first order in g/Δ, we have

$$\begin{aligned} UH_{JC}U^\dagger \approx{}& \omega_c a^\dagger a + \xi e^{-i(\tilde{\Omega}t+\tilde{\phi}_0)} a^{\dagger 2} + \xi e^{i(\tilde{\Omega}t+\tilde{\phi}_0)} a^2 \\ &+ \sum_{j=1}^{2}\left[\frac{\tilde{\omega}_a}{2} + \frac{4g^2}{\Delta^2}(\xi e^{-i(\tilde{\Omega}t+\tilde{\phi}_0)} a^{\dagger 2} + \text{H.c.}) \right. \\ &\left. + \frac{4g^2}{\Delta} a^\dagger a\right]\sigma_z^{(j)} + \sum_{j=1}^{2}\left[\left(\frac{2g\xi e^{-i(\tilde{\Omega}t+\tilde{\phi}_0)}}{\Delta} a^\dagger \right.\right. \\ &\left.\left. + \frac{g^2 \xi e^{-i(\tilde{\Omega}t+\tilde{\phi}_0)}}{\Delta^2}\right)\sigma_+^{(j)} + \text{H.c.}\right] \\ &+ \mu_1(e^{-i(\tilde{\Omega}t+\tilde{\phi}_0)}\sigma_+^{(1)}\sigma_+^{(2)} + e^{i(\tilde{\Omega}t+\tilde{\phi}_0)}\sigma_-^{(1)}\sigma_-^{(2)}) \\ &+ \mu_2(\sigma_+^{(1)}\sigma_-^{(2)} + \sigma_-^{(1)}\sigma_+^{(2)}), \end{aligned}$$

where

$$\tilde{\omega}_a = E_J(\Phi_x) + 4g^2/\Delta,$$

$$\mu_1 = 2g^2\xi/\Delta^2, \quad \mu_2 = g^2/\Delta.$$

By adiabatically eliminating the degrees of freedom of the resonator, the following two-qubit Hamiltonian can be obtained:

$$H_A \approx \sum_{j=1}^{2}\frac{E_J(\Phi_x)}{2}\sigma_z^{(j)} + \mu_2(\sigma_+^{(1)}\sigma_-^{(2)} + \sigma_-^{(1)}\sigma_+^{(2)})$$

$$+ \mu_1(e^{-i(\tilde{\Omega}t+\tilde{\phi}_0)}\sigma_+^{(1)}\sigma_+^{(2)} + e^{i(\tilde{\Omega}t+\tilde{\phi}_0)}\sigma_-^{(1)}\sigma_-^{(2)}).$$

Here, we have omitted all the single-qubit terms induced by the interaction between qubits and the resonator because of the conditions

$$E_J(\Phi_x)/2 \gg g^2/\Delta, \xi g/\Delta.$$

As analyzed in Sec. V A, we can continuously adjust the parameter ξ, thus the coupling strength μ_1 is continuously tunable.

Since the two superconducting charge qubits also interact with the uncontrollable degrees of freedom in the environment (e.g., quantum noises induced by charge fluctuations on the electric gates), the discussed two-qubit system should be considered as an open quantum system. For this two-qubit system, the master Eq. (2) can be obtained under the Born-Markov approximation [26]. From Eq. (19), at the charge degenerate points for both qubits, we know that the optimal concurrence $C_{\max}\approx 0.31$ and fidelity $F_{\max}\approx 0.65$ can be obtained when

$$\tilde{\Omega} = 2E_J(\Phi_x), \quad \xi = \frac{1}{\sqrt{5}+1}\frac{\Delta^2}{g^2}\Gamma_1.$$

Using now the same experimental parameters from Ref. [26]:

$$\Delta = E_J - \omega_r = 5 \text{ GHz} - 4.8 \text{ GHz} = 200 \text{ MHz},$$

$$g = 20 \text{ MHz}, \quad \Gamma_1/2\pi \sim 0.1 \text{ MHz},$$

$$\lambda_g, \lambda_e \sim 10 \text{ MHz}, \quad \delta \sim 100 \text{ MHz},$$

the squeezed amplitude ξ is of the order of 1 MHz, which can be realized by a strong microwave driving field with coupling strength $\lambda_d \sim 100$ MHz. These parameters show that our entanglement-production proposal is experimentally realizable.

Although this section mainly concentrates on how to prepare entangled states in two charge qubits coupled to a transmission line resonator, our proposal is also extendable to two flux qubits in a coplanar transmission line resonator [51]. Since the system parameters [51] are almost of the same order of those for charge qubits, there is no essential difference between them, as far as applying our proposal.

VI. CONCLUSIONS

In summary, we study the stationary entanglement for two-qubit systems, each qubit with independent decoherence channels. We discussed two scenarios: (i) no time-dependent field or (ii) a time-dependent field is applied to the two-qubit system. We find that by tuning the single-qubit and two-qubit parameters a maximum concurrence of the stationary entangled states is about 0.31 and a maximum fidelity between the maximally entangled states and the stationary state is about 0.65 for such two-qubit system.

It should be noted that the detuning between the frequencies of the two qubits should be large enough for scenario (i), so that the nonrotating term cannot be neglected. However, for scenario (ii), the frequency of the time-dependent field should match the sum of the frequencies of the two qubits. Thus, the nonrotating term is naturally kept. The qubit with the highest frequency might excite the higher energy levels of the qubit with lower frequency for case (i), or the time-dependent field might excite the higher energy levels of both qubits for case (ii). To make the two-level approximation valid, we assume that the transition frequency from the first excited state to the second excited state satisfies either the condition in Eq. (9) for case (i), or the condition in Eq. (17) for case (ii). These conditions can be satisfied in physical systems.

As examples, we apply our general theory to several different superconducting quantum circuits. For two supercon-

ducting qubits coupled strongly via an inductive or a capacitive element, one can tune the stationary entanglement by varying either the single-qubit oscillating frequencies or the coupling strengths between the qubits. For superconducting qubits weakly coupled via a quantum cavity (e.g., a transmission line resonator), an auxiliary superconducting three-level system [38,39] with Δ-shaped transition is introduced to induce a controllable squeezed field in the cavity. Such a controllable quantum squeezed field can be further used to entangle two qubits in open environments.

Even though the proposed strategy can be used to produce stationary entanglement, the obtained entanglement may not be high enough to be used in quantum information processing. Additional entanglement purification processes (e.g., [41]) should be introduced to increase the stationary entanglement. These procedures could make the superconducting circuit too complex. For this reason, further research (possibly using the methods in Ref. [52]) will be focused on modifying our proposal to obtain higher stationary entanglement.

Another interesting problem would be to develop a short-time regime dissipation-induced entanglement production strategy, e.g., to investigate the entanglement production when the decoherence and dissipation effects cannot be omitted during the gate operation process. In this regime, the correlation effects of the environmental noises should be considered, which leads to non-Markovian noises [53]. Different effects may be produced under non-Markovian noises. The existing decoherence suppression strategies [54,55] against non-Markovian noises may be helpful to solve this problem.

ACKNOWLEDGMENTS

F.N. acknowledges partial support from the National Security Agency (NSA), Laboratory Physical Science (LPS), Army Research Office (USARO), National Science Foundation (NSF) Grant No. EIA-0130383, and JSPS-RFBR Grant No. 06-02-91200. J.Z. was supported by the National Natural Science Foundation of China under Grants No. 60704017, No. 60433050, No. 60635040, and No. 60674039 and the China Postdoctoral Science Foundation. T.J.T. would also like to acknowledge partial support from the U.S. Army Research Office under Grant No. W911NF-04-1-0386.

APPENDIX: DERIVATION OF THE MAXIMUM CONCURRENCE AND FIDELITY

In this appendix, we show the derivation of the concurrence C of the stationary state ρ_∞ and the fidelity F between ρ_∞ and the maximally entangled state ρ_m. Thus, we will derive Eq. (6) in the main text.

In order to simplify our discussions, let us use the so-called coherent vector picture as in Refs. [56,57]. Considering the inner product $\langle X,Y\rangle=\mathrm{tr}(X^\dagger Y)$, we can find the following matrix basis for all two-qubit matrices:

$$\left\{\frac{1}{2}I_{4\times4},\Omega_{14}^{x},\Omega_{14}^{y},\Omega_{23}^{x},\Omega_{23}^{y},\frac{1}{2}\sigma_{x}^{(1)},\frac{1}{2}\sigma_{y}^{(1)},\frac{1}{2}\sigma_{x}^{(2)},\frac{1}{2}\sigma_{y}^{(2)},\frac{1}{2}\sigma_{x}^{(1)}\sigma_{z}^{(2)},\frac{1}{2}\sigma_{z}^{(1)}\sigma_{x}^{(2)},\frac{1}{2}\sigma_{y}^{(1)}\sigma_{z}^{(2)},\frac{1}{2}\sigma_{z}^{(1)}\sigma_{y}^{(2)},\Omega_{14}^{z},\Omega_{23}^{z},\frac{1}{2}\sigma_{z}^{(1)}\sigma_{z}^{(2)},\right\} \tag{A1}$$

where $I_{4\times4}$ is the 4×4 identity matrix, and Ω_{14}^{x}, Ω_{14}^{y}, Ω_{23}^{x}, Ω_{23}^{y}, Ω_{14}^{z}, and Ω_{23}^{z} are defined as

$$\Omega_{14}^{x}=\begin{pmatrix} & & & \frac{1}{\sqrt{2}} \\ & & 0 & \\ & 0 & & \\ \frac{1}{\sqrt{2}} & & & \end{pmatrix},\quad \Omega_{14}^{y}=\begin{pmatrix} & & & \frac{-i}{\sqrt{2}} \\ & & 0 & \\ & 0 & & \\ \frac{i}{\sqrt{2}} & & & \end{pmatrix},$$

$$\Omega_{23}^{x}=\begin{pmatrix} & & & 0 \\ & & \frac{1}{\sqrt{2}} & \\ & \frac{1}{\sqrt{2}} & & \\ 0 & & & \end{pmatrix},\quad \Omega_{23}^{y}=\begin{pmatrix} & & & 0 \\ & & \frac{-i}{\sqrt{2}} & \\ & \frac{i}{\sqrt{2}} & & \\ 0 & & & \end{pmatrix},$$

$$\Omega_{14}^z = \begin{pmatrix} \frac{1}{\sqrt{2}} & & & \\ & 0 & & \\ & & 0 & \\ & & & \frac{-1}{\sqrt{2}} \end{pmatrix}, \quad \Omega_{23}^z = \begin{pmatrix} 0 & & & \\ & \frac{1}{\sqrt{2}} & & \\ & & \frac{-1}{\sqrt{2}} & \\ & & & 0 \end{pmatrix}.$$

The system density matrix ρ can be expanded under this matrix basis as

$$\rho = \frac{1}{4} I_{4\times 4} + \sum_{i=1}^{15} m_i \Omega_i,$$

where $\Omega_i (i=1,\ldots,15)$ are all traceless basis matrices in Eq. (A1) and $m_i = \mathrm{tr}(\Omega_i \rho)$.

Let $m=(m_1,\ldots,m_{15})^T$, and thus the master Eq. (2) can be rewritten as [56,57]

$$\dot{m} = O_A m + Dm + g, \tag{A2}$$

where O_A is the adjoint representation matrix of $-iH_A$ and $(Dm+g)$ is the coherent vector representation of the Lindblad terms

$$\sum_{j=1}^{2} \Gamma_1 \mathcal{D}[\sigma_{-j}]\rho + \sum_{j=1}^{2} 2\Gamma_\phi [\sigma_{zj}]\rho,$$

with $D \le 0$ and g a constant vector. Further, let

$$m^p = (m_{14}^x, m_{14}^y, m_{23}^x, m_{23}^y)^T,$$

$$m^\eta = (m_{14}^z, m_{23}^z, m_{zz})^T,$$

$$m^\epsilon = (m_{x0}, m_{y0}, m_{0x}, m_{0y}, m_{xz}, m_{zx}, m_{yz}, m_{zy})^T,$$

where

$$m_{14}^\alpha = \mathrm{tr}(\Omega_{14}^\alpha \rho), \quad m_{23}^\beta = \mathrm{tr}(\Omega_{23}^\beta \rho), \quad \alpha,\beta = x,y,z,$$

$$m_{\alpha\beta} = \mathrm{tr}\left[\left(\frac{1}{2}\sigma_\alpha^{(1)}\sigma_\beta^{(2)}\right)\rho\right], \quad \alpha,\beta = 0,x,y,z,$$

and $\sigma_0^{(j)} = I_{2\times 2} (j=1,2)$ are 2×2 identity matrices acting on the qubit j. Then, we can rewrite Eq. (A2) as

$$\dot{m}^p = O_0^p m^p + \sum_{i=1}^{4} u_i O_i^\eta m^\eta + D^p m^p,$$

$$\dot{m}^\eta = \sum_{i=1}^{4} u_i (-O_i) m^p + D^\eta m^\eta + g^\eta,$$

$$\dot{m}^\epsilon = \sum_{i=1}^{4} u_i O_i^\epsilon m^\epsilon + D^\epsilon m^\epsilon, \tag{A3}$$

where $D^p = -4(\Gamma_1 + 2\Gamma_\phi) I_{4\times 4} = -8\Gamma_2 I_{4\times 4}$ and

$$u_1 = 8\mu_1 \cos\theta_1, \quad u_2 = 8\mu_1 \sin\theta_1,$$

$$u_3 = 8\mu_2 \cos\theta_2, \quad u_4 = -8\mu_2 \sin\theta_2,$$

$$O_0^p = \begin{pmatrix} 0 & \Omega & & \\ -\Omega & 0 & & \\ & & 0 & \omega_{a1}-\omega_{a2} \\ & & \omega_{a2}-\omega_{a1} & 0 \end{pmatrix},$$

$$O_1^\eta = \begin{pmatrix} 0 & 0 & 0 \\ -1 & 0 & 0 \\ 0 & 0 & 0 \\ 0 & 0 & 0 \end{pmatrix}, \quad O_2^\eta = \begin{pmatrix} 1 & 0 & 0 \\ 0 & 0 & 0 \\ 0 & 0 & 0 \\ 0 & 0 & 0 \end{pmatrix},$$

$$O_3^\eta = \begin{pmatrix} 0 & 0 & 0 \\ 0 & 0 & 0 \\ 0 & 0 & 0 \\ 0 & -1 & 0 \end{pmatrix}, \quad O_4^\eta = \begin{pmatrix} 0 & 0 & 0 \\ 0 & 0 & 0 \\ 0 & 1 & 0 \\ 0 & 0 & 0 \end{pmatrix},$$

$$D^\eta = \begin{pmatrix} -4\Gamma_1 & 0 & 0 \\ 0 & -4\Gamma_1 & 0 \\ 4\sqrt{2}\Gamma_1 & 0 & -8\Gamma_1 \end{pmatrix}, \quad g^\eta = \begin{pmatrix} 2\sqrt{2}\Gamma_1 \\ 0 \\ 0 \end{pmatrix}. \tag{A4}$$

D^ϵ and O_i^ϵ in the last equation in Eq. (A3) are, respectively, negative and traceless skew-symmetric matrices.

With simple calculations, we can obtain the following stationary solution of Eq. (A3):

$$m^\epsilon(\infty) = 0, \quad m_{23}^x(\infty) = m_{23}^y(\infty) = m_{23}^z(\infty) = 0,$$

$$m_{14}^x(\infty) = \frac{1}{\sqrt{2}} p \cos(\theta_1 - \phi), \quad m_{14}^y(\infty) = \frac{1}{\sqrt{2}} p \sin(\theta_1 - \phi),$$

$$m_{14}^z(\infty) = \frac{\sqrt{2}}{4}\left\{1 + \sqrt{1 - \frac{8\Gamma_2}{\Gamma_1} p^2}\right\},$$

$$m_{zz}(\infty) = \frac{1}{4}\left\{1 + \sqrt{1 - \frac{8\Gamma_2}{\Gamma_1} p^2}\right\},$$

where p and ϕ are given in Eq. (5), from which we can calculate the stationary state ρ_∞ and the stationary fidelity

$F(\rho_\infty)$ in Eq. (6).

Further, recall that the concurrence of the quantum state

$$\rho = \begin{pmatrix} a & & & w \\ & b & z & \\ & z^* & c & \\ w^* & & & d \end{pmatrix}$$

can be analytically solved as [58]

$$C(\rho) = 2\ \max\{|w| - \sqrt{bc}, |z| - \sqrt{ad}, 0\},$$

from which we can obtain the stationary concurrence $C(\rho_\infty)$ in Eq. (6).

[1] Y. Makhlin, G. Schön, and A. Shnirman, Rev. Mod. Phys. **73**, 357 (2001).

[2] G. Wendin and V. S. Shumeiko, *Handbook of Theoretical and Computational Nanoscience* (Forschungszentrum Karlsruhe, Germany, 2005); e-print arXiv:cond-mat/0508729.

[3] J. Q. You and F. Nori, Phys. Today **58** (11), 42 (2005).

[4] J. Clarke and F. K. Wilhelm, Nature (London) **453**, 1031 (2008).

[5] Yu. A. Pashkin, T. Yamamoto, O. Astafiev, Y. Nakamura, D. Averin, and J. Tsai, Nature (London) **421**, 823 (2003).

[6] T. Yamamoto, Yu. A. Pashkin, O. Astafiev, Y. Nakamura, and J. Tsai, Nature (London) **425**, 941 (2003).

[7] A. J. Berkley, H. Xu, R. C. Ramos, M. A. Gubrud, F. W. Strauch, P. R. Johnson, J. R. Anderson, A. J. Dragt, C. J. Lobb, and F. C. Wellstood, Science **300**, 1548 (2003).

[8] A. Izmalkov, M. Grajcar, E. Ilichev, Th. Wagner, H. G. Meyer, A. Yu. Smirnov, M. H. S. Amin, A. Maassen van den Brink, and A. M. Zagoskin, Phys. Rev. Lett. **93**, 037003 (2004).

[9] J. B. Majer, F. G. Paauw, A. C. J. terHaar, C. J. P. M. Harmans, and J. E. Mooij, Phys. Rev. Lett. **94**, 090501 (2005).

[10] R. McDermott, R. W. Simmonds, M. Steffen, K. B. Cooper, K. Cicak, K. D. Osborn, S. Oh, D. P. Pappas, and J. M. Martinis, Science **307**, 1299 (2005).

[11] T. Hime, P. A. Reichardt, B. L. T. Plourde, T. L. Robertson, C. E. Wu, A. V. Ustinov, and J. Clarke, Science **314**, 1427 (2006); I. Siddiqi and J. Clarke, *ibid.* **313**, 1400 (2006).

[12] Y. X. Liu, L. F. Wei, J. S. Tsai, and F. Nori, Phys. Rev. Lett. **96**, 067003 (2006); G. S. Paraoanu, Phys. Rev. B **74**, 140504(R) (2006).

[13] P. R. Johnson, F. W. Strauch, A. J. Dragt, R. C. Ramos, C. J. Lobb, J. R. Anderson, and F. C. Wellstood, Phys. Rev. B **67**, 020509(R) (2003).

[14] J. Li, K. Chalapat, and G. S. Paraoanu, Phys. Rev. B **78**, 064503 (2008).

[15] S. Ashhab, A. O. Niskanen, K. Harrabi, Y. Nakamura, T. Picot, P. C. de Groot, C. J. P. M. Harmans, J. E. Mooij, and F. Nori, Phys. Rev. B **77**, 014510 (2008); S. Ashhab and F. Nori, *ibid.* **76**, 132513 (2007); S. Ashhab, S. Matsuo, N. Hatakenaka, and F. Nori, *ibid.* **74**, 184504 (2006); C. Rigetti, A. Blais, and M. Devoret, Phys. Rev. Lett. **94**, 240502 (2005).

[16] Y. Makhlin, G. Schön, and A. Shnirman, Nature (London) **398**, 305 (1999).

[17] Y. X. Liu, C. P. Sun, and F. Nori, Phys. Rev. A **74**, 052321 (2006); C. M. Wilson, T. Duty, F. Persson, M. Sandberg, G. Johansson, and P. Delsing, Phys. Rev. Lett. **98**, 257003 (2007).

[18] H. Xu, F. W. Strauch, S. K. Dutta, P. R. Johnson, R. C. Ramos, A. J. Berkley, H. Paik, J. R. Anderson, A. J. Dragt, C. J. Lobb, and F. C. Wellstood, Phys. Rev. Lett. **94**, 027003 (2005).

[19] K. Xia, M. Macovei, J. Evers, C. H. Keitel, Phys. Rev. B **79**, 024519 (2009).

[20] R. Migliore and A. Messina, Phys. Rev. B **72**, 214508 (2005).

[21] S. H. W. van der Ploeg, A. Izmalkov, A. M. van den Brink, U. Hübner, M. Grajcar, E. Il'ichev, H. G. Meyer, and A. M. Zagoskin, Phys. Rev. Lett. **98**, 057004 (2007).

[22] Y. D. Wang, P. Zhang, D. L. Zhou, and C. P. Sun, Phys. Rev. B **70**, 224515 (2004); L. F. Wei, Y. X. Liu, and F. Nori, *ibid.* **71**, 134506 (2005).

[23] A. T. Sornborger, A. N. Cleland, and M. R. Geller, Phys. Rev. A **70**, 052315 (2004); M. R. Geller and A. N. Cleland, *ibid.* **71**, 032311 (2005); E. J. Pritchett and M. R. Geller, *ibid.* **72**, 010301(R) (2005); F. Xue, Y. D. Wang, C. P. Sun, H. Okamoto, and H. Yamaguchi, N. J. Phys. **9**, 35 (2007).

[24] J. Q. You and F. Nori, Phys. Rev. B **68**, 064509 (2003); J. Q. You, J. S. Tsai, and F. Nori, *ibid.* **68**, 024510 (2003); Y. X. Liu, L. F. Wei, and F. Nori, Europhys. Lett. **67**, 941 (2004).

[25] M. Wallquist, V. S. Shumeiko, and G. Wendin, Phys. Rev. B **74**, 224506 (2006); M. Paternostro, M. S. Tame, G. M. Palma, and M. S. Kim, Phys. Rev. A **74**, 052317 (2006).

[26] A. Blais, J. Gambetta, A. Wallraff, D. I. Schuster, S. M. Girvin, M. H. Devoret, and R. J. Schoelkopf, Phys. Rev. A **75**, 032329 (2007).

[27] Y. X. Liu, L. F. Wei, J. R. Johansson, J. S. Tsai, and F. Nori, Phys. Rev. B **76**, 144518 (2007); M. Grajcar, Y. X. Liu, F. Nori, and A. M. Zagoskin, *ibid.* **74**, 172505 (2006); X. L. He, Y. X. Liu, J. Q. You, and F. Nori, Phys. Rev. A **76**, 022317 (2007); X. L. He, J. Q. You, Y. X. Liu, L. F. Wei, and F. Nori, Phys. Rev. B **76**, 024517 (2007).

[28] L. F. Wei, Y. X. Liu, and F. Nori, Phys. Rev. Lett. **96**, 246803 (2006); L. F. Wei, Y. X. Liu, M. J. Storcz, and F. Nori, Phys. Rev. A **73**, 052307 (2006).

[29] D. Braun, Phys. Rev. Lett. **89**, 277901 (2002); F. Benatti, R. Floreanini, and M. Piani, *ibid.* **91**, 070402 (2003).

[30] S. Nicolosi, A. Napoli, A. Messina, and F. Petruccione, Phys. Rev. A **70**, 022511 (2004).
[31] L. M. Duan and G. C. Guo, Phys. Rev. Lett. **79**, 1953 (1997); P. Zanardi and M. Rasetti, *ibid.* **79**, 3306 (1997); D. A. Lidar, I. L. Chuang, and K. B. Whaley, *ibid.* **81**, 2594 (1998); L. A. Wu and D. A. Lidar, *ibid.* **88**, 207902 (2002).
[32] A. R. R. Carvalho, F. Mintert, S. Palzer, and A. Buchleitner, Eur. Phys. J. D **41**, 425 (2007).
[33] A. J. Berkley, H. Xu, M. A. Gubrud, R. C. Ramos, J. R. Anderson, C. J. Lobb, and F. C. Wellstood, Phys. Rev. B **68**, 060502(R) (2003).
[34] H. Xu, A. J. Berkley, R. C. Ramos, M. A. Gubrud, P. R. Johnson, F. W. Strauch, A. J. Dragt, J. R. Anderson, C. J. Lobb, and F. C. Wellstood, Phys. Rev. B **71**, 064512 (2005).
[35] J. M. Martinis, S. Nam, J. Aumentado, K. M. Lang, and C. Urbina, Phys. Rev. B **67**, 094510 (2003).
[36] D. F. Walls and G. J. Milburn, *Quantum Optics* (Springer-Verlag, Berlin, 1994).
[37] W. K. Wootters, Phys. Rev. Lett. **80**, 2245 (1998).
[38] Y. X. Liu, J. Q. You, L. F. Wei, C. P. Sun, and F. Nori, Phys. Rev. Lett. **95**, 087001 (2005); F. Deppe, M. Mariantoni, E. P. Menzel, A. Marx, S. Saito, K. Kakuyanagi, H. Tanaka, T. Meno, K. Semba, H. Takayanagi, E. Solano, and R. Gross, Nat. Phys. **4**, 686 (2008).
[39] J. Q. You, Y. X. Liu, C. P. Sun, and F. Nori, Phys. Rev. B **75**, 104516 (2007).
[40] C. H. Bennett, G. Brassard, S. Popescu, B. Schumacher, J. A. Smolin, and W. K. Wootters, Phys. Rev. Lett. **76**, 722 (1996); W. Dür and H. J. Briegel, Rep. Prog. Phys. **70**, 1381 (2007).
[41] K. Maruyama and F. Nori, Phys. Rev. A **78**, 022312 (2008); T. Tanamoto, K. Maruyama, Y. X. Liu, X. Hu, and F. Nori, *ibid.* **78**, 062313 (2008).
[42] F. Gaitan, Phys. Rev. B **63**, 104511 (2001); V. Plerou and F. Gaitan, *ibid.* **63**, 104512 (2001).
[43] O. Astafiev, Yu. A. Pashkin, Y. Nakamura, T. Yamamoto, and J. S. Tsai, Phys. Rev. Lett. **93**, 267007 (2004).
[44] P. Bertet, I. Chiorescu, G. Burkard, K. Semba, C. J. P. M. Harmans, D. P. DiVincenzo, and J. E. Mooij, Phys. Rev. Lett. **95**, 257002 (2005).
[45] J. Q. You, J. S. Tsai, and F. Nori, Phys. Rev. Lett. **89**, 197902 (2002); T. Yamamoto, M. Watanabe, J. Q. You, Yu. A. Pashkin, O. Astafiev, Y. Nakamura, F. Nori, and J. S. Tsai, Phys. Rev. B **77**, 064505 (2008).
[46] C. J. Villas-Boas, N. G. de Almeida, R. M. Serra, and M. H. Y. Moussa, Phys. Rev. A **68**, 061801(R) (2003); N. G. de Almeida, R. M. Serra, C. J. Villas-Boas, and M. H. Y. Moussa, *ibid.* **69**, 035802 (2004).
[47] X. Hu and F. Nori, Phys. Rev. Lett. **76**, 2294 (1996); **79**, 4605 (1997); Phys. Rev. B **53**, 2419 (1996); Physica B **263**, 16 (1999).
[48] X. Hu, Ph.D. thesis, University of Michigan (UM), 1996; see also http://www-personal.umich.edu/~nori/squeezed.html
[49] M. J. Everitt, T. D. Clark, P. B. Stiffell, A. Vourdas, J. F. Ralph, R. J. Prance, and H. Prance, Phys. Rev. A **69**, 043804 (2004).
[50] A. M. Zagoskin, E. Il'ichev, M. W. McCutcheon, J. Young, and F. Nori, Phys. Rev. Lett. **101**, 253602 (2008).
[51] T. Lindstrom, C. H. Webster, J. E. Healey, M. S. Colclough, C. M. Muirhead, and A. Ya. Tzalenchuk, Supercond. Sci. Technol. **20**, 814 (2007).
[52] M. Zhang, H. Y. Dai, Z. R. Xi, H. W. Xie, and D. W. Hu, Phys. Rev. A **76**, 042335 (2007).
[53] W. T. Strunz, L. Diosi, and N. Gisin, Phys. Rev. Lett. **82**, 1801 (1999); T. Yu, Phys. Rev. A **69**, 062107 (2004).
[54] G. Gordon, N. Erez, and G. Kurizki, J. Phys. B **40**, S75 (2007); L. Viola and S. Lloyd, Phys. Rev. A **58**, 2733 (1998); G. Ithier, E. Collin, P. Joyez, P. J. Meeson, D. Vion, D. Esteve, F. Chiarello, A. Shnirman, Y. Makhlin, J. Schriefl, and G. Schön, Phys. Rev. B **72**, 134519 (2005).
[55] W. Cui, Z. R. Xi, and Y. Pan, Phys. Rev. A **77**, 032117 (2008).
[56] R. Alicki and K. Lendi, *Quantum Dynamical Semigroup and Applications* (Springer-Verlag, New York, 1985).
[57] C. Altafini, J. Math. Phys. **44**, 2357 (2003); J. Zhang, C. W. Li, R. B. Wu, T. J. Tarn, and X. S. Liu, J. Phys. A **38**, 6587 (2005); J. Zhang, R. B. Wu, C. W. Li, T. J. Tarn, and J. W. Wu, Phys. Rev. A **75**, 022324 (2007).
[58] T. Yu and J. H. Eberly, Phys. Rev. Lett. **93**, 140404 (2004); T. Yu and J. H. Eberly, *ibid.* **97**, 140403 (2006).